Controlled defects and enhanced electronic extraction in fluorine-incorporated zinc oxide for high-performance planar perovskite solar cells

Wenjing Zhao, Hua Li, Zhike Liu, Dapeng Wang*, Shengzhong (Frank) Liu*

Key Laboratory of Applied Surface and Colloid Chemistry, Ministry of Education, Shaanxi Key Laboratory for Advanced Energy Devices, Shaanxi Engineering Lab for Advanced Energy Technology, School of Materials Science and Engineering, Shaanxi Normal University, Xi'an 710119, China

ARTICLE INFO

ABSTRACT

Oxygen-related defects in the intrinsic metal-oxide films restrict the transportation and collection processes of photogenerated carriers from the perovskite film to charge transport layers, which obstruct the applications of metal-oxide films in perovskite solar cells (PSCs). In this study, fluorine as an anion dopant was introduced to modify the oxygen-related defects in the intrinsic zinc oxide (ZnO). The impact of fluorine concentration on the structural, electrical, and optical characteristics of solution-processed ZnO films was systematically investigated. When the fluorine concentration was optimized to 15%, fluorine-doped ZnO (ZnO:F) film exhibited multiple advantageous effects, such as large crystalline size, low oxygen-related defect state density, good hydrophobic surface, and high conductivity. Furthermore, ZnO:F films with various fluorine concentrations as electron transport layers (ETLs) were introduced into the PSCs. The PSCs based on the ZnO:F ETL with the fluorine concentration of 15% yielded a maximum power conversion efficiency of 16.23% owing to the improvements of short-circuit current and fill factor. Meanwhile, the thermochemical stability of the device based on the ZnO:F ETL was also significantly improved.

1. Introduction

Organic-inorganic halide perovskite materials exhibit the superior optoelectronic properties [1–5], including tunable bandgaps, high absorption coefficients, small exciton binding energies, low charge recombination rates, and long charge carrier diffusion lengths, enabling low-cost, high efficiency, simple-processing photovoltaic devices. Recently, the most advanced perovskite solar cells (PSCs) achieve a certified power conversion efficiency (PCE) of > 22% by virtue of the development of perovskite active layer materials [6,7], various processing techniques [8,9], and device architectures, which is approaching the PCE of commercial thin-film solar cells like cadmium telluride and silicon.

In a typical photovoltaic device architecture, the perovskite absorber layer is usually sandwiched between an electron transport layer (ETL) and a hole transport layer (HTL). In case of a PSC with high-efficiency, the ETL plays an indispensable role in blocking holes and transporting electrons. On the other hand, the ETL also can effectively separate the perovskite absorber layer from the elecotrode to reduce the direct recombination of photo-induced carriers. In case of the ETL, several kinds of n-type metal oxide semiconductors, such as TiO_2 [10–12], ZnO [13–15], SnO_2 [16], and In_2O_3 [17], have been

considered as the promising candidates for electron transport materials. Among them, TiO_2 is one of most robust and stable ETL for the state-of-the-art PSCs. Undoubtedly, ZnO is an absolutely predominant candidate to replace TiO_2 applied as the ETL in the PSCs because of its comparable energy levels as well as high electron mobility [18]. Despite impressive properties from using ZnO ETL, many native defects of ZnO should be well considered, especially for oxygen vacancies (V_O). It is noted that the high defect state density originated from V_O in metal oxide ETLs is harmful to the charge extraction and transportation in PSCs.

In comparison with binary oxide, ZnO-based ternary oxides have been widely investigated as ETLs for PSC application, such as Al–ZnO [19], Mg–ZnO [20], Ti–ZnO [21], and Li–ZnO [22]. Several possible functions of metal-cation based-ternary oxide ETLs have been proposed for the improvement of the performance of PSCs: adjusting the energy level to promote electron injection from the perovskite layer into the ETLs, reducing the defect state density of ETLs to suppress charge recombination and enhance electron transport, and modifying the morphology of ETLs and even affect the quality in the perovskite or at the ETLs/perovskite interface. However, to obtain the high-performance PSCs, the nonmetal-anion doped ZnO as ETLs have been rarely investigated. Fluorine (F), as a halogen family element, is a promising anion doping candidate because its ionic radius (1.36 Å) is similar to

---

that of oxygen (1.40 Å) [23]. The high size-compatibility of their ionic radius effectively reduces the lattice distortion compared with metal-cation dopants. In addition, F can occupy the V_O sites in the ZnO atomic structure to form the stronger zinc−fluorine (Zn–F) bonds (364 kJ/mol) compared with the zinc−oxygen (Zn–O) bonds (284 kJ/mol) [24], which contributing to the enhancement of thermal stability. Moreover, the substitution of an oxygen ion (O^{2-}) with a fluorine ion (F^-) supplies a free election because of the difference in the electro-valence of O^{2-} and F^- [25], resulting in the increase in the conductivity of F-doped ZnO film. On the basis of the above-mentioned advantages for F-incorporated ZnO, it is expected that F-doped ZnO as ETL is capable of controlling defects and improving electronic properties for high performance PSCs applications.

In this study, F as an anion dopant was introduced to modify the oxygen-related defects in the intrinsic ZnO. The impact of F concentration on the structural, electrical, and optical characteristics of solution-processed ZnO films was systematically investigated. In case of the F concentration was 15%, F-doped ZnO (ZnO:F) film exhibited large crystalline size, low oxygen-related defect state density, good hydrophobic surface, and high conductivity. Furthermore, ZnO:F films with various F concentrations were introduced into the PSCs as ETLs. The PSCs based on the ZnO:F ETL with an optimal F concentration of 15% yielded to a maximum power conversion efficiency (PCE) of 16.23%. More significantly, the thermochemical stability of the device based on the ZnO:F ETL with F concentration of 15% was remarkably enhanced.

2. Experimental

The pristine and F-doped ZnO films were formed onto chemically cleaned fluorine-doped tin oxide-coated (FTO) glass by sol-gel spin-coating. These solutions with various fluorine concentrations were prepared by dissolving the zinc precursor of zinc acetate dihydrate (Zn(CH$_3$COO)$_2$·H$_2$O) and the dopant precursor of ammonium fluoride (NH$_4$F) in 2-methoxyethanol; monoethanolamine (MEA) as a stabilizer was added into the solutions. The molar ratios of reactant to MEA were controlled at 1:1, and the ion concentrations were set consistently to 0.35 M. The corresponding concentration ratios of F to Zn in the solutions were varied from 0% to 20%, in graduations of 5%. The transparent and homogeneous solutions can be obtained after heating at 60 °C for 2 h. After cooling down to room temperature, the solutions were aged for 1 day. The solutions were subsequently fabricated onto the FTO substrates at 4000 rpm for 40 s. To evaporate the solvent and remove the organic residuals, the substrates were annealed at 300 °C for 10 min. The films were prepared according to the above-mentioned processes two times, and were then annealed in air at 500 °C for 1 h. Finally, the pristine and F-doped ZnO films with a thickness of ~80 nm were obtained.

Following by the fabrication of solution-processed ZnO:F ETLs, the CH$_3$NH$_3$PbI$_3$ perovskite absorber layer was made as follows. Firstly, a mixture perovskite precursor solution was prepared at room temperature in glove box, including 0.461 g PbI$_2$ (99.99%, Alfar Aesar) and 0.159 g CH$_3$NH$_3$I dissolved in a 71 μL dimethylsulfoxide (DMSO) and 633 μL dimethylformamide (DMF). After the filtration, the mixed solution is spin-coated on the ETLs at 4000 rpm for 30 s and methylbenzene as anti-solvent was dripped into the precursor solution during the spin-coating process. At last, the dark perovskite films were obtained after post-annealing on a hot-plate at 100 °C for 10 min. For the HTL solution, 90 mg spiroMeOTAD, 28.8 μL tert-butylpyridine, and 22 μL lithium bis imide acetonitrile solution (520 mg/mL) were dissolved in 1 mL chlorobenzene. The HTL solution was also spin-coated onto perovskite layer at 4000 rmp for 30 s. Au electrode with a thickness of 80 nm was then deposited by a thermal evaporator. Finally, the PSC structure of FTO/undoped or F-doped ZnO/CH$_3$NH$_3$PbI$_3$/spiroMeOTAD/Au was obtained.

The surface morphology and roughness images of the pristine and F-doped ZnO films were characterized by a field-emission scanning electron microscopy (SEM, HITACHI, SU 8020) and an atomic force microscope (AFM, Brooke, Dimension ICON). The chemical properties of the ZnO-related films were investigated by XPS (ESCALAB250Xi, Thermo Fisher Scientific). Photoluminescence (PL) and time-resolved PL (TRPL) were carried out with an Edinburgh Instruments Ltd. FLS980 spectrometer. The PL excitation source is a picosecond pulsed diode laser at 325 nm with a pulse width of 64.2 ps. The TRPL was measured using 405 nm beam for photon excitation with the PL peak at 760 nm. All decays were measured with a 4096-channel analyzer. The photocurrent density versus voltage (J–V) performance of the PSCs were measured by using a Keithley 2400 source meter under the solar simulator illumination with the light intensity of 100 mW/cm^2 (AM 1.5 G, SAN-EIELECTRIC XES-40S2-CE solar simulator), as calibrated by a NREL-traceable KG5 filtered silicon reference cell. The active area of all solar cells was prepared by a 9×9 mm^2 mask. All devices were measured under the standard test procedure at a scan rate of 30 mV/s. Incident photon-to-current conversion efficiency (IPCE) spectra of the PSCs were recorded by a QTest Station 500TI system (Crowntech. Inc., USA). The monochromatic light intensity for IPCE was calibrated using a reference silicon detector.

3. Results and discussion

The XRD patterns of the pristine and F-doped ZnO films are shown in Fig. 1a. It is clear that the (002) diffraction peak, the c-axis of the crystal lattice, is oriented highly perpendicular to the substrate plane for all films. A weak XRD peak corresponding to the plane (101) is also observed for the pristine ZnO film. When the various F concentrations are introduced into ZnO film, the (101) peak completely vanishes. As shown in Fig. 1b, the (002) diffraction peak position shifts from 34.19° for the pristine ZnO film to 34.49° for the ZnO:F with F concentration of 5%, and further increases gradually to 34.54° for the ZnO:F with F
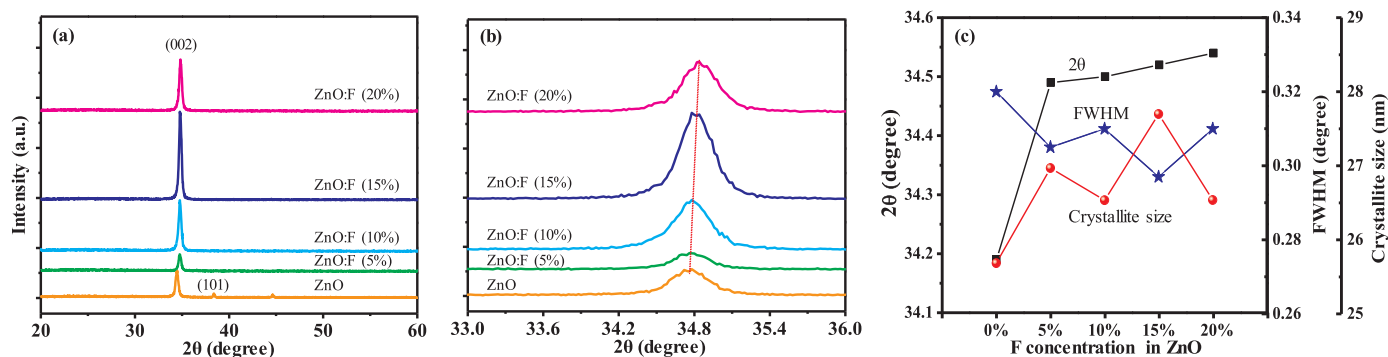

Fig. 1. (a) XRD patterns and (b) the enlarged (002) peak of the pristine and F-doped ZnO films fabricated with various F concentrations, and (c) variation in 2θ, FWHM, and crystallite size of the pristine and F-doped ZnO films.